EUROPEAN ORGANISATION FOR NUCLEAR RESEARCH (CERN)

October 17, 2024

Addendum to the NA61/SHINE Proposal: Request for high-statistics p+p measurements in Run 3

The NA61/SHINE Collaboration

This document presents the NA61/SHINE request for four weeks of hadron beam time on the H2 beam line for physics data taking in 2025. The requested high-statistics data set will be used to measure proton-proton correlations and the differential production cross sections of deuterons, antideuterons, and antiprotons in p+p interactions at 300 GeV/c with NA61/SHINE across a wide y–p_{T} range. These high-impact measurements will significantly advance the understanding of cosmic antinuclei.

CERN-SPSC-2024-028 / SPSC-P-330-ADD-15
18/10/2024

Contents

Executive Summary

In recent years, the AMS-02 Collaboration has reported detecting several cosmic antideuteron candidate events in the energy region of a few GeV per nucleon (GeV/n) [6–12]. It is an open question if the explanation of these events require an explanation invoking new physics, like dark matter annihilation or decay [2, 4, 13–35], or can be attributed to known astrophysical processes (Fig. 1). The objective of this addendum is to collect high-statistics p+p data at 300 GeV/c with NA61/SHINE to build a state-of-the-art model with significantly reduced uncertainties to conclusively determine if the events can be explained by conventional astrophysical background.

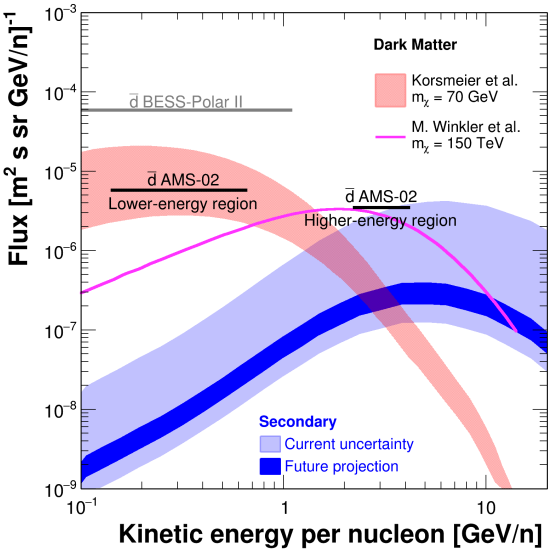

Figure 1: Predicted antideuteron flux from different dark matter annihilation models (red, magenta) [1–3]) and secondary astrophysical background (blue) [4]. The width of the red dark matter band indicates the uncertainty in antideuteron formation. The magenta line shows a model motivated by the AMS-02 antihelium candidates [3]. The width of the light-blue band indicates the current uncertainty in antideuteron propagation and formation, and the dark-blue band indicates the projected reduced uncertainty based on this addendum's p+p data at 300 GeV/c. The black lines denote the projections down to which flux level current AMS-02 data can exclude antideuterons [5].

The astrophysical background flux of antideuterons is predominantly produced through proton interactions with interstellar hydrogen and helium gas. The antideuteron production cross section increases while the cosmic proton flux decreases with energy. Consequently, cosmic antideuteron production peaks at a laboratory momentum (p_{lab}) of about 300 GeV/c in p+p interactions. Currently, the uncertainties in the production of astrophysical antideuteron background are on the order of a factor of 10, i.e., they range from approximately one-tenth to ten times the predicted values. Direct measurement of antideuteron production in p+p interactions is statistically very challenging with existing datasets in the SPS energy range. However, the proposed data set enables constructing a new state-of-the-art antideuteron model from the source size of p+p interactions (Fig. 2, right) and antiproton differential production cross sections. This model will also be validated by directly measuring the deuteron and antideuteron production cross sections, reducing the antideuteron production uncertainty by a factor of 5. These measurements will be accomplished by collecting approximately 600 M p+p interactions at 300 GeV/c using the upgraded fixed-target experiment NA61/SHINE. The number of collisions will be an order of magnitude greater than the currently available data sets in the energy range most relevant to cosmic rays. The measurement can be achieved with four weeks of hadron beam at 300 GeV/c on a liquid hydrogen target.

Initial source size estimates using p–p correlation measurements in the existing NA61/SHINE data set, comprising 60 M p+p events at 158 GeV/c, relies on only about 180 identified p–p

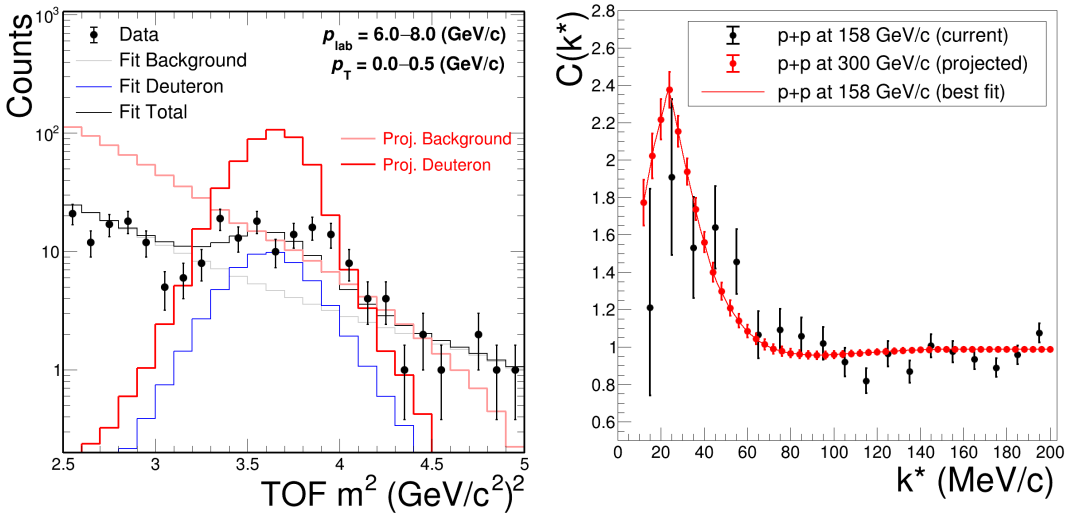

Figure 2: Left: Mass template fit showing the fitted deuteron peak and background in *p*+*p* 158 GeV/*c* data and the projected improvements in the deuteron fit with the proposed *p*+*p* 300 GeV/*c* data. **Right:** *p*–*p* correlation function as a function of k^*, the relative momentum of the proton pair in the pair center-of-mass frame, for existing *p*+*p* 158 GeV/*c* data set (points) along with the projected uncertainty band for the proposed 300 GeV/*c* *p*+*p* measurement.

pairs in the low-k^* peak. k^* represents the relative momentum in the pair center-of-mass frame. The proposed data at 300 GeV/*c*, with improved particle identification power, is projected to contain about 2,000 *p*–*p* pairs in the low-k^* region, thereby reducing the total uncertainty in the source size by about a factor of 5. Crucially, the new production model will be validated using the same dataset, with precision deuteron measurements and the first-ever antideuteron production measurements in this energy range. About 200 deuterons have been identified in the existing *p*+*p* data set at 158 GeV/*c* (Fig. 5, left). The proposed data set is projected to identify approximately 3,000 deuteron tracks and measure them as a function of rapidity and transverse momentum. This will facilitate the first precision measurement of deuteron production in *p*+*p* interactions as a function of rapidity and transverse momentum at SPS energies. In the same dataset, a few antideuteron candidate tracks were identified (Fig. 5, right). For the proposed data set, about 100 antideuteron tracks are expected to be identified. This will be the first antideuteron production cross section measurements in *p*+*p* interactions at cosmic-ray energies. The preliminary antiproton production uncertainties (Fig. 4, left) in the same *p*+*p* 158 GeV/*c* data (statistical uncertainty of approximately 10% and a systematic uncertainty of approximately 20%) are currently too large to effectively reduce the uncertainties in modeling astrophysical antideuterons [36–38]. The proposed data set aims to provide antiproton production measurements in rapidity-transverse momentum bins with an improved statistical uncertainty of approximately 3% and a systematic uncertainty of approximately 10% [39] (Sec. 3).

In summary, the significantly improved measurements with NA61/SHINE are critical for evaluating the hypothesized dark matter origin of the AMS-02 antideuteron candidates.

1 Physics Motivation

1.1 Motivation and Experimental Status

Space-based and balloon-borne experiments, like BESS, PAMELA, and AMS-02 [40–47] have been searching for rare cosmic antinuclei because they might be crucial messengers of new-physics phenomena in the Galaxy. In a wide range of viable dark matter models [2, 4, 13–35], cosmic antinuclei are predicted to provide a "smoking gun" signature of dark matter annihilation or decay (Fig. 1). When there is no clear dark matter signal in any experiment, broadening the search with different techniques and messengers is a priority. In contrast to direct dark matter searches, *i.e.* dark matter scattering experiments, which are most sensitive to couplings of dark matter to nuclei [48], dark matter searches with antinuclei are also sensitive to additional models, e.g., dark-photon or heavy dark matter models. The Snowmass 2021 Cross Frontier Report [49] concluded: "Low-energy cosmic-ray antideuterons as a possible new low-background discovery channel, address a current gap in sensitivity in the MeV gamma-ray band, provide new tests of sterile neutrino DM, and more generally enhance our sensitivity to DM across a very broad range of energy scales and cosmic messengers." Antinuclei have up to three orders of magnitude lower astrophysical backgrounds resulting from interactions of primary cosmic rays with the interstellar medium (ISM) compared to production in a wide range of dark matter models (Fig. 1). This is a crucial advantage compared to searches with positrons (e.g., [50–52]), antiprotons (e.g., [40–43, 45]), or γ-rays (e.g., [53, 54]).

The AMS-02 experiment is sensitive to antideuterons in two distinct kinetic energy regions, resulting from two different subdetectors for the velocity reconstruction. AMS-02 reports seven antideuteron candidates for the higher-energy region (several GeV) [6], which could be a signal from dark matter annihilation (e.g., [3]). However, in this energy range the significance of these candidates depends on the astrophysical antideuteron background uncertainties because many models predict a similar level of antideuterons from dark matter annihilation or decay and astrophysical production [2, 4, 13–21, 27, 32–35]. Therefore, reducing the background uncertainties is paramount for the higher-energy region. For example, at a kinetic energy of 3 GeV/n, the antideuteron signal predicted by a model [3] (Fig. 1, magenta line) overlaps with the current best prediction of the background antideuteron flux. The proposed measurements enable confirming or ruling out if the AMS-02 higher energy antideuterons are of astrophysical-background origin.

1.2 Antinuclei Formation Uncertainties

Significant uncertainties, on the order of a factor of 10, in the production model hinder the interpretation of higher-energy AMS-02 antideuteron candidates. These uncertainties must be reduced to conclusively determine whether they originate from astrophysical backgrounds. The astrophysical background antinuclei flux is dominantly produced in proton interactions with the interstellar hydrogen and helium gas. The cosmic proton flux decreases, while the antinuclei production cross section increases with energy [55]. This means that p+p collision measurements in the range of $p_{\mathrm{lab}} = 50 - 400$ GeV/c are the most relevant for reducing uncertainties when interpreting antideuteron candidates in AMS-02's higher-energy region. The

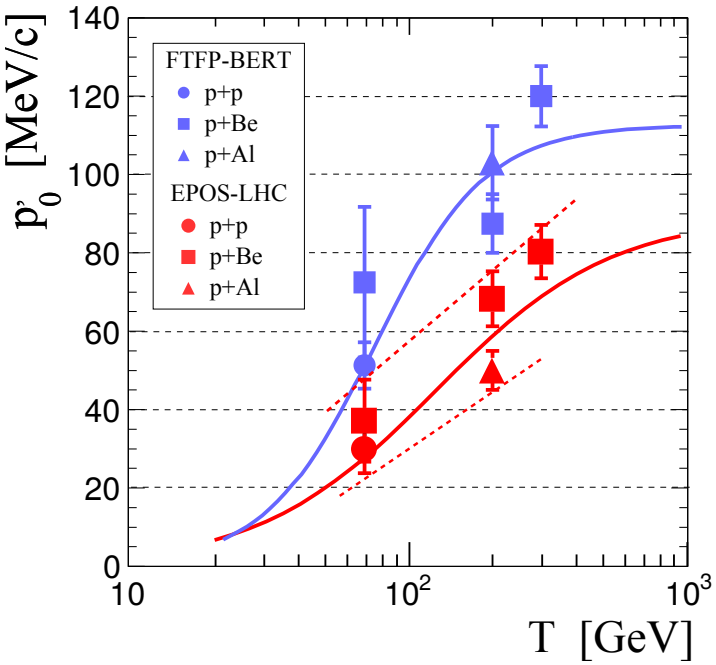

Figure 3: Coalescence momentum p_0' for antideuterons as a function of the kinetic energy of the incoming proton for two different hadronic generators. p_0' accounts for the discrepancies in antiproton production by current hadronic generators, which affect the coalescence momentum p_0. The solid lines show empiric fits to the best-fit p_0' values for the corresponding generator. The dashed red lines indicate the one-sigma uncertainty range for EPOS-LHC [56].

following gives a brief overview of several antinuclei production models. As the underlying physics is equally applicable to both nuclei and antinuclei formation, the term "(anti)nuclei" refers to both unless otherwise specified.

1.2.1 Coalescence Model

The most frequently used production model in cosmic-ray applications is the simple coalescence model in which any pair of (anti)proton ($\bar{p}$) and (anti)neutron ($\bar{n}$) within a sphere of radius p_0 in momentum space will coalesce to produce an antinucleus. This model links the (anti)proton $N_{\bar{p}}$ and (anti)neutron $N_{\bar{n}}$ yields to the (anti)deuteron yield $N_{\bar{d}}$:

$$E_{\bar{d}}\frac{\mathrm{d}^3N_{\bar{d}}}{\mathrm{d}p_{\bar{d}}^3} = \underbrace{\frac{8\pi}{3}\frac{p_0^3}{m_{\bar{p}}}}_{=B_2}\left(E_{\bar{p}}\frac{\mathrm{d}^3N_{\bar{p}}}{\mathrm{d}p_{\bar{p}}^3}\right)\left(E_{\bar{n}}\frac{\mathrm{d}^3N_{\bar{n}}}{\mathrm{d}p_{\bar{n}}^3}\right), \tag{1}$$

with E_X and p_X being the corresponding energies and momenta and $m_{\bar{p}}$ the (anti)proton mass. As typical hadronic generators [57–63] do not produce (anti)deuterons, an event-by-event coalescence approach applying the condition $k^* = |\vec{p}_{\bar{p}} - \vec{p}_{\bar{n}}|/2 < p_0$ to $\bar{p}$–$\bar{n}$-pairs simulated with hadronic generators in their respective center-of-mass frame was used in a series of studies [4, 20, 55, 56, 64]. From fits to data, the phenomenological quantity coalescence momentum p_0 is determined to be about 100 MeV/c, which is smaller than the typical scale for

perturbative QCD to break down, indicating sensitivity to non-perturbative effects [56]. This quantity not only describes the difference in momenta of coalescing (anti)nucleons but also encompasses various other effects, such as antinucleon spectra mismatch and source size. Data from p+p, p+Al, and p+Be collisions were used for a system-independent fit to model the coalescence momentum as a function of energy. Figure 3 illustrates a steep increase in the coalescence momentum between 100–400 GeV, the most relevant region for cosmic rays. Crucial limitations of this study are that results between p+Al and p+Be vary by about 2σ and that the fit is heavily impacted by only one existing older p+p measurements at 70 GeV with significant uncertainties [65]. For the same 70 GeV data, antideuterons and deuterons demonstrate an unexpected inconsistency in the fitted coalescence momentum, leading to additional concerns in the validity of this data set [56]. Given these factors and the third-power influence of p_0' on B_2, it is a conservative assumption that the total antideuteron yield has an uncertainty greater than a factor of 10. Figure 3 also shows a general discrepancy between different hadronic models, with Geant4 FTFP-BERT being above EPOS-LHC by about 50–100%.

A more advanced coalescence approach uses the femtoscopic extraction of the p+p interaction source size from correlation measurements to build a model that considers the interaction source shape, interaction potential, and the antideuteron wave function [66–70]. Many shortcomings of the simple coalescence model (Sec. 1.2) are addressed by using an alternative definition for B_2 in Eq. (1) [71–73]:

$$B_2(p_\mathrm{T}) \approx \frac{3}{2m_{\bar{d}}} \int \mathrm{d}^3 q D(q) \exp\left(-R(p_\mathrm{T})^2 q^2\right), \tag{2}$$

with $D(q) = \int \mathrm{d}^3 r |\phi_d(r)|^2 \exp(-iqr)$ and q is the relative momentum. This has the advantage that it takes into account the interaction source size $R(p_\mathrm{T})$ as a function of the antideuteron's transverse momentum p_T and the antideuteron's internal wave function $\phi_d(r)$. Following the ALICE approach [74, 75], the source size can be femtoscopically extracted from the two-proton correlation function:

$$C(k^*) = \mathcal{N} \cdot \frac{N_\mathrm{same}(k^*)}{N_\mathrm{mixed}(k^*)}, \tag{3}$$

with $N_\mathrm{same}(k^*)$ and $N_\mathrm{mixed}(k^*)$ being the distributions of correlated and uncorrelated proton pairs, respectively, and $\mathcal{N}$ being a normalization factor. The interaction source size can then be determined from a fit to the correlation function by using the following definition:

$$C(k^*) = \int \mathrm{d}^3 r S(r) |\Psi(r, k^*)|^2, \tag{4}$$

with $S(r)$ being the emission source function and $\Psi(r, k^*)$ being the two-proton wave function that is the result of solving the Schrödinger equation for a two-proton interaction potential (e.g., with CATS [76]). Using the measured source size, ALICE successfully described their antideuteron data with a Gaussian antideuteron wavefunction and an Argonne-v_{18} potential for the two-proton interaction potential [70].

1.2.2 Other Models

Additional models for (anti)nuclei production exist. For instance, the production of (anti)nuclei in p+p collisions can be discussed in a thermal model approach, with the hadronization happening in so-called fireballs [77–79]. All products of the fireball continue interacting with each other until the mean free path for elastic collisions is larger than the system size (freeze-out) [71]. Furthermore, the multi-phase transport AMPT model [80], initially developed for heavy-ion collisions, was successfully applied to describe antinuclei production in p+p at RHIC and ALICE energies and the production threshold [81, 82]. In general, examining particle yield measurements in p+p interactions over a large phase space range enables discriminating between different model predictions. However, this is severely limited by the availability of p+p data and their significant uncertainties in the momentum range relevant to cosmic antideuterons. It also has to be noted that measurements in heavy-ion collisions or at high energies [83–104] are less applicable to evaluate cosmic antideuteron candidates because these interactions are subdominant in the Galaxy.

1.3 Reducing Uncertainties in Antideuteron Production Modeling with NA61/SHINE

NA61/SHINE is the only operational experiment capable of confirming or ruling out whether the AMS-02 higher-energy antideuteron candidates originate from interactions of primary cosmic rays with the ISM. The goal of reducing uncertainties in cosmic antideuteron production modeling will be achieved through analyzing p–p correlations and measuring deuteron production cross sections in proton–liquid hydrogen target interactions, and the first-ever measurements of antideuteron production cross sections in this energy range. While these are the main focus, the addendum will also improve upon previous measurements of the antiproton differential production cross sections, an essential byproduct of the analysis of the proposed data set. Collectively, these four elements are critical for improving the prediction power of cosmic antideuteron production models. The most relevant momentum range for p+p measurements is $p_{\text{lab}} = 50 - 400$ GeV/c, making NA61/SHINE the ideal experiment for interpreting cosmic-ray antinuclei.

The foundation and motivation for the proposed high-statistics measurement at 300 GeV/c are the results with limited statistics from the 158 GeV/c p+p data, which will be discussed in Sec. 1.3.1–1.3.4. In the same way, as for the 158 GeV/c data, the $\sim$6$\times$ smaller already recorded 400 GeV/c p+p data set (11 M), currently under calibration, will also be analyzed. However, to interpret the reported cosmic antideuteron candidates, the uncertainty in cosmic antideuteron background modeling must be reduced by approximately a factor of 5. This requires significantly enhanced measurements of the system source size and the deuteron and antiproton differential production cross sections. These necessary improvements can be achieved with the proposed 600 M p+p events at 300 GeV/c with the upgraded NA61/SHINE detector.

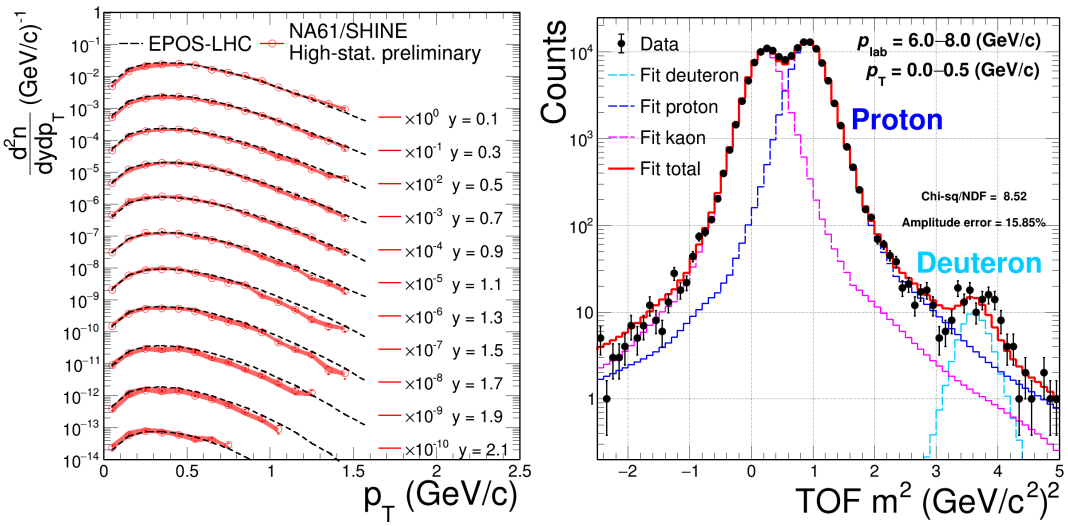

Figure 4: Left: New preliminary antiproton spectra (in red) as a function of transverse momentum in rapidity slices in inelastic p+p interactions at 158 GeV/c. The systematic uncertainties are represented as a band and amount to approximately 20%. Statistical uncertainties are around 10%. **Right:** Mass template fit showing clear proton, kaon, and deuteron peaks in p+p 158 GeV/c data.

1.3.1 Antiproton Yield Measurement

The combined 2009/2010/2011 high-statistics 60 M-p+p 158 GeV/c data set was already used to perform production cross section measurements for antiprotons and protons and is in the preliminary release stage with an envisioned publication in 2024. The dE/dx in the Time Projection Chambers (TPCs) was used for particle identification in bins of transverse momentum and rapidity (Fig. 4, left). The results extend the prior p_T and kinetic energy ranges, based on the 2009 p+p data alone, of the produced antiprotons by a factor of ~2 [105]. Compared to the low-statistics results from NA61/SHINE for the same energy [106], these new results reduce the statistical uncertainties by more than a factor of 3. It was found that the EPOS-LHC model overestimates the antiproton production by 10–20% [39]. This substantially affects the modeling of the cosmic antideuteron background. As shown in Eq. (1), assuming isospin symmetry, the antideuteron production models rely on the square of the antiproton yield. Therefore, reducing uncertainties in antiproton production measurements is a crucial objective.

1.3.2 Deuteron Yield Measurement

The same data were used to measure the deuteron production yield in this p+p energy range for the first time in a modern precision experiment. The Time-of-Flight (ToF) measurements were used together with the dE/dx from the TPCs to extract deuteron yields. The right panel of Fig. 4 shows a mass template fit, indicating a clear deuteron contribution. This technique makes the deuteron measurement possible in the momentum range 4–8 GeV/c. Approximately 200 deuteron tracks have been identified in the p+p 158 GeV/c data sets. The

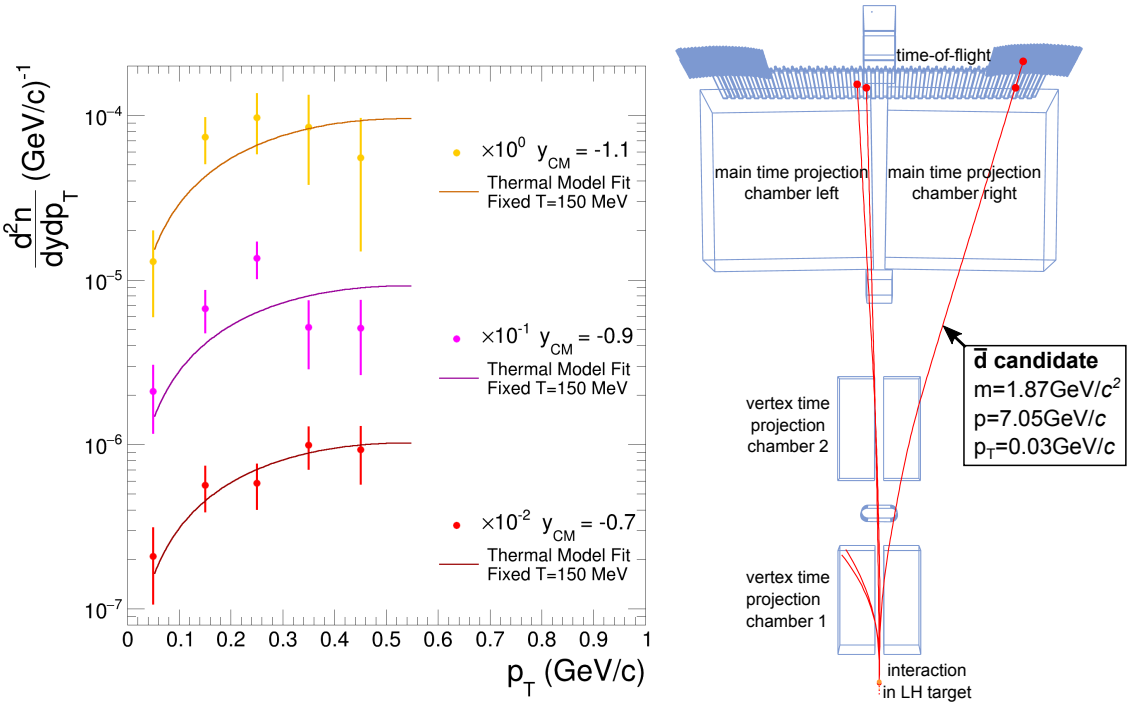

Figure 5: Left: Work-in-progress deuteron spectra as a function of transverse momentum in rapidity slices in inelastic p+p interactions at 158 GeV/c. Systematic uncertainties are not shown. Solid lines show the overlaid two-parameter thermal model with the shape parameter set to $T = 150$ MeV (from [106]) prior to the fit. Only the amplitude parameter was fitted to the data. Comparisons with the EPOS-LHC model [57] are shown in black. **Right:** NA61/SHINE detector with an antideuteron candidate in p+p 158 GeV/c data.

work-in-progress deuteron spectra, which include corrections for detector background, acceptance, and efficiencies, are shown in (Fig. 5, left). Deuteron production in this momentum range is dominated by interactions like $pp \to d\bar{n}p$, with the coalescence formation mechanism for this channel being identical to the antideuteron production channel ($pp \to \bar{d}nppp$). A significant quantity is the d/p ratio, which is a decisive quantity that distinguishes between different production models and impacts the modeling.

1.3.3 Antideuteron Yield Measurement

In p+p collisions at cosmic-ray energies, the production of antideuterons is approximately 1,000 times smaller than that of antiprotons [55]. The ToF-d$E/$dx analysis of negatively-charged tracks in the existing p+p 158 GeV/c data sets has yielded several antideuteron candidate events. Fig. 5 (right) illustrates a p+p collision event featuring an antideuteron candidate. For the proposed data set, it is anticipated that about 100 antideuterons will be identified, facilitating the first-ever measurements of antideuteron production cross section in p+p interactions at cosmic-ray energies. These measurements are expected to achieve a statistical uncertainty of ~70% and a systematic uncertainty of ~50% in the $p_{\text{lab}} = 5 - 10\,\text{GeV}/c$ range.

1.3.4 Source Size Measurement

Two-proton correlation studies have been measured at high energies (e.g., ALICE [75]), but no accepted theory exists to predict the source size at low energies. NA61/SHINE has conducted correlation studies before, but either without particle identification [107, 108] or for pions [109], which are easier to identify than protons. The 158 GeV/c p+p data enable determining the source size from proton pairs in this energy range for the first time, making it a crucial result to complement RHIC and ALICE measurements at high energies. The right panel of Fig. 2 demonstrates the initial $C(k^*)$ measurement status. Proton pairs were extracted from the data, ensuring that protons from detector interactions and Λ decays are suppressed to a minimum. The result shows a clear difference from a uniform distribution, and a provisional correlation function fit suggests a source size of 1–2 fm. However, the statistics are low, and only about 180 proton-proton pairs have been identified in the low-k^* region. Increasing the number of identified proton pairs is essential to reduce the statistical uncertainties that currently dominate the uncertainties in the extracted source size of the system.

The ultimate goal of measuring the interaction source size and the antiproton differential production cross section is to construct a data-driven (anti)deuteron coalescence model. The model will be validated by comparing its predictions with the precision deuteron yield measured from the same data set and by cross-checking these predictions against the first-ever antideuteron measurements in this energy range. The 158 GeV/c data provides the first proof that a model for (anti)deuteron production can be constructed using such measurements.

1.4 Additional Outcomes

Other NA61/SHINE working groups can also utilize the proposed dataset. It will enable the study of $\Xi^{\pm}$ and Ω production in p+p interactions at SPS energies, offering critical insights into strangeness production in nucleus-nucleus collisions. The high-statistics dataset will allow the examination of $\Xi^{\pm}$ production as a function of produced particle multiplicity at SPS energies. Additionally, it will benchmark critical point-sensitive fluctuations by extending reference high-statistics measurements of multiplicity and net-charge fluctuations in p+p reaction between $\sqrt{s_{\mathrm{NN}}}$ = 17.3 and 27.4 GeV [110, 111].

2 Planned Measurements

2.1 Experimental Setup

A schematic layout of the NA61/SHINE detector system is shown in Fig. 6. The main components of the detection system are four large-volume Time Projection Chambers (TPC). Two of them, called Vertex TPCs (VTPC-1, VTPC-2), are located downstream of the target inside superconducting magnets. The main TPCs (MTPCs) detectors are placed symmetrically to the beamline downstream of the magnets. A Gap TPC and a set of three forward TPCs (FTPCs) improve acceptance for high-momentum forward-going tracks. In addition, two

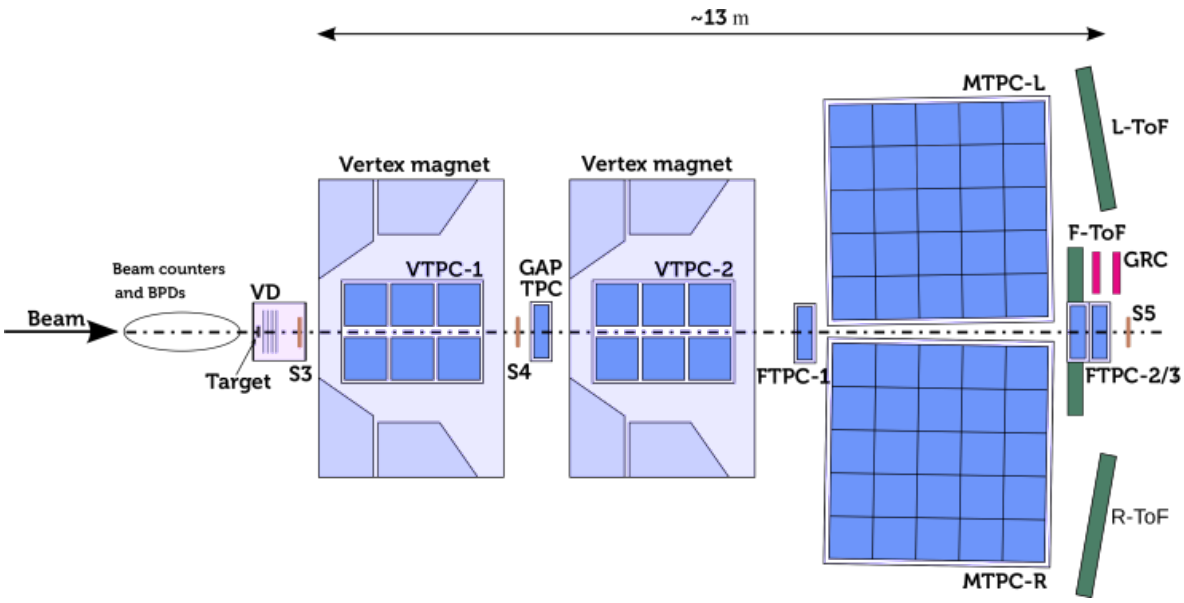

Figure 6: Schematic view of the NA61/SHINE experimental setup, which will be used for the proposed measurements.

walls of pixel Time-of-Flight detectors (ToF-L and ToF-R) are downstream of the MTPC-L and MTPC-R.

During CERN Long Shutdown 2, significant improvements to TPC backend electronics resulted in a reduction of noise and a factor of ~2 improvement in the $\mathrm{d}E/\mathrm{d}x$ resolution. Also, the replacement of the readout electronics increased the data-taking rate to 2 kHz (~20× faster). New ToF detectors with $\sigma_t = 80$ ps [112, 113] were installed, and additional detectors increased the acceptance for highly forward-boosted tracks.

2.2 Liquid Hydrogen Target

For data taking on p+p interactions, a liquid hydrogen target (LHT) with a length of 20.29 cm (2.8% interaction length) and a diameter of 3 cm will be placed upstream of VTPC-1. The target is filled with para-hydrogen obtained in a closed-loop liquefaction system and operates at 75 mbar overpressure relative to the atmosphere. At the atmospheric pressure of 965 mbar, the liquid hydrogen density is $\rho_{LH} = 0.07$ g/cm^3. The boiling rate in the liquid hydrogen is not monitored during the data collection, and thus, the liquid hydrogen density is only approximately known. Data taking with the liquid hydrogen target inserted and removed is planned to calculate a data-based correction for interactions with material surrounding the liquid hydrogen.

2.3 Data Taking Conditions

Data is expected to be recorded under the following conditions:

- SPS cycle length: from 26.4 s to $\approx$ 70 s, flat top: $\approx$ 5 s, average duty cycle: $\approx$ 0.15,
- Fraction of wanted hadrons (protons) within secondary beam hitting the NA61/SHINE target: 90%,
- Maximum intensity of the secondary beam: 200 kHz,
- Target: 2.8% interaction probability,
- Recorded event rate during the spill: 1500 Hz,
- Fraction of time for physics data taking (includes planned and unplanned detector and machine interruptions): $\approx$ 80%,
- Mean of the number of recorded events: $\approx$ 23 M events/day.

The mean number of recorded p+p collisions after off-line quality cuts (mostly off-time beam rejection) and reduction due to contamination of off-target interactions will be about 18 M events/day.

Approximately 600 M p+p events can be recorded during four weeks of data taking.

2.4 Beam Request

Given the presented ideas in this document, the NA61/SHINE Collaboration requests a hadron beam time of four weeks on the H2 beam line for physics data taking in 2025. This time will be used to make essential high-statistics p+p measurements with NA61/SHINE at 300 GeV/c, significantly impacting the understanding of cosmic antinuclei, quark-gluon plasma, and critical point searches.

3 Physics Performance

During the NA61/SHINE system size-energy scan, p+p reactions were collected at six different energies. The largest statistics, approximately 60 M p+p interactions at 158 GeV/c, were recorded in 2009, 2010, and 2011. The analysis of this dataset provides the foundation for the proposed measurements. The current status of systematic and statistical uncertainties of the 158 GeV/c data and the projected uncertainties of the proposed measurements at 300 GeV/c are shown in Table 1.

A p+p dataset approximately 10$\times$ larger (600 M events), collected with the upgraded NA61/SHINE detector at 300 GeV/c – compared to the previously discussed 158 GeV/c dataset – will provide new measurements of protons–proton correlations, antiprotons, and deuterons. This proposed dataset will feature significantly reduced systematic and statistical uncertainties, enhancing our ability to discriminate between different nuclear formation models. Systematic uncertainties, influenced by the $\mathrm{d}E/\mathrm{d}x$ resolution in the TPCs, are expected to halve due to a 2$\times$ improvement in $\mathrm{d}E/\mathrm{d}x$ resolution in the upgraded TPCs, along with an enhancement in the ToF resolution from 120 ps to approximately 80 ps. Similarly, statistical uncertainties are projected to decrease significantly due to a 10$\times$ increase in the number of

Table 1: Current and Projected Uncertainties in Measurements

Measurement	Current uncertainties		Projected uncertainties	
	Statistical	**Systematic**	**Statistical**	**Systematic**
p–p correlations	25%	20%	10%	10%
Deuteron differential cross section	50%	30%	15%	15%
Antiproton differential cross section	10%	20%	3%	10%
Antideuteron differential cross section	n/a	n/a	70%	50%

recorded p+p collisions and enhanced particle production resulting from the slight increase in available energy ($\sqrt{s}$) from 17.3 GeV to 23.8 GeV. The following proposed measurements will significantly benefit from the upgraded detector with 20$\times$ faster readout, enabling the data-taking goals to be accomplished in ~1 month:

- The new data is projected to contain about 2,000 p–p pairs in the low-k^* region, enabling the first precision femtoscopic measurement of the p+p source size in this energy range (Fig. 2, right).
- The proposed data set is projected to make deuteron measurements possible in the expanded momentum range of 4–12 GeV/c, effectively doubling the momentum range for deuteron measurements. These improvements will lead to about 3,000 identified deuterons. Fig. 2 (left) demonstrates this improvement in one of the phase space bins. Together with the lower-statistics measurements at 158 GeV/c and 400 GeV/c, the new high-statistics measurements will enable discriminating between various deuteron formation models.
- Precision antiproton production measurements in rapidity-transverse momentum bins with an improved statistical uncertainty of approximately 3% and a systematic uncertainty of approximately 10% will be provided.
- It is anticipated that about 100 antideuterons will be identified in the range of 4–8 GeV/c.

Combining these four items will allow building, testing, and validating data-driven deuteron and antideuteron production models in the energy range most relevant to cosmic rays. This will reduce uncertainties in the astrophysical background modeling of antideuterons by

about a factor of 5. This directly enables evaluating the origin of the higher-energy AMS-02 antideuteron candidates (Fig. 1).

4 Summary

This addendum requests beam time at the upgraded NA61/SHINE facility for crucial measurements in high-statistics p+p interactions at 300 GeV/c (approximately 10$\times$ larger (600 M events) than the previously analyzed 158 GeV/c dataset): p–p correlations, deuteron production cross sections, and the first-ever antideuteron production cross section in this energy range. Additionally, it will be used to measure antiproton production cross sections with unprecedented precision. Together, these measurements will be instrumental in building and validating a state-of-the-art model for the production of astrophysical antideuterons. The anticipated reduction in systematic and statistical uncertainties is crucial for refining cosmic antideuteron production models. This breakthrough is essential for understanding the origins of the AMS-02 high-energy antideuteron candidates. Taking this dataset in 2025 offers a unique opportunity before Long Shutdown 3.

References

[1] A. Cuoco, J. Heisig, M. Korsmeier, and M. Krämer *Journal of Cosmology and Astroparticle Physics* **1710** no. 10, (2017) 053, arXiv:1704.08258 [astro-ph.HE].

[2] M. Korsmeier, F. Donato, and N. Fornengo *Physical Review D* **97** no. 10, (2018) 103011, arXiv:1711.08465 [astro-ph.HE].

[3] M. W. Winkler, P. D. L. T. Luque, and T. Linden *Physical Review D* **107** no. 12, (June, 2023) . http://dx.doi.org/10.1103/PhysRevD.107.123035.

[4] L. Š erkšnytė, S. Königstorfer, P. von Doetinchem, L. Fabbietti, D. M. Gomez-Coral, J. Herms, A. Ibarra, T. Pöschl, A. Shukla, A. Strong, and I. Vorobyev *Physical Review D* **105** no. 8, (Apr, 2022) . https://doi.org/10.1103%2Fphysrevd.105.083021.

[5] A. Oliva *https://indico.cern.ch/event/1400721/contributions/6037459/attachments/2913061/5111478/20240820%20-%20AMS%20Overview%20-%20A.%20Oliva.pdf*, *August 20* (2024) .

[6] Y.-H. Chang, "Cosmic Anti-Deuterons," in *44th COSPAR Scientific Assembly. Held 16-24 July*, vol. 44, p. 2082. July, 2022.

[7] S. Ting *Press Conference at CERN, December 8* (2016) .

[8] S. Ting *Colloquium at CERN, May 24* (2018) .

[9] A. Kounine *Next Generation of AstroParticle Experiments in Space (NextGAPES-2019)* *http://www.sinp.msu.ru/contrib/NextGAPES/files/AMS_AK.pdf*, *June 21* (2019) .

[10] A. Oliva *https://indico.cern.ch/event/849055/contributions/3598085/attachments/1925619/3187261/01_LAN2019_-_Observations_of_cosmic-rays_and_search_for_anti-nuclei_with_AMS-02_-_A._Oliva.pdf*, *October 14* (2019) .

[11] V. Choutko, "Cosmic Heavy Anti-Matter," in *44th COSPAR Scientific Assembly. Held 16-24 July*, vol. 44, p. 2083. July, 2022.

[12] S. Ting *Colloquium at CERN, Jun 8* *https://indico.cern.ch/event/1275785/* (2023) .

[13] F. Donato, N. Fornengo, and P. Salati *Physical Review D* **62** (2000) 043003, arXiv:hep-ph/9904481 [hep-ph].

[14] H. Baer and S. Profumo *Journal of Cosmology and Astroparticle Physics* **0512** (2005) 008, arXiv:astro-ph/0510722 [astro-ph].

[15] R. Duperray, B. Baret, D. Maurin, G. Boudoul, A. Barrau, L. Derome, K. Protasov, and M. Buénerd *Physical Review D* **71** no. 8, (Apr., 2005) 083013, astro-ph/0503544.

[16] F. Donato, N. Fornengo, and D. Maurin *Physical Review D* **78** (2008) 043506, arXiv:0803.2640 [hep-ph].

[17] C. B. Bräuninger and M. Cirelli *Physics Letters B* **678** (2009) 20–31, arXiv:0904.1165 [hep-ph].

[18] Y. Cui, J. D. Mason, and L. Randall *Journal of High Energy Physics* **1011** (2010) 017, arXiv:1006.0983 [hep-ph].

[19] A. Ibarra and S. Wild *Journal of Cosmology and Astroparticle Physics* **1302** (2013) 021, arXiv:1209.5539 [hep-ph].

[20] A. Ibarra and S. Wild *Physical Review D* **88** (2013) 023014, arXiv:1301.3820 [astro-ph.HE].

[21] N. Fornengo, L. Maccione, and A. Vittino *Journal of Cosmology and Astroparticle Physics* **1309** (2013) 031, arXiv:1306.4171 [hep-ph].

[22] D. Cerdeño, M. Peiró, and S. Robles *Journal of Cosmology and Astroparticle Physics* **1408** (2014) 005, arXiv:1404.2572 [hep-ph].

[23] L. Dal and A. Raklev *Physical Review D* **89** (2014) 103504, arXiv:1402.6259 [hep-ph].

[24] M. Cirelli, N. Fornengo, M. Taoso, and A. Vittino *Journal of High Energy Physics* **1408** (2014) 009, arXiv:1401.4017 [hep-ph].

[25] E. Carlson, A. Coogan, T. Linden, S. Profumo, A. Ibarra, and S. Wild *Physical Review D* **89** no. 7, (Apr., 2014) 076005, arXiv:1401.2461 [hep-ph].

[26] A. Hryczuk, I. Cholis, R. Iengo, M. Tavakoli, and P. Ullio *Journal of Cosmology and Astroparticle Physics* **1407** (2014) 031, arXiv:1401.6212 [astro-ph.HE].

[27] T. Aramaki *et al. Physics Reports* **618** (Mar., 2016) 1–37, arXiv:1505.07785 [hep-ph].

[28] N. Tomassetti and A. Oliva *Proceedings of Science* **EPS-HEP2017** (2017) 620, arXiv:1712.03177 [astro-ph.HE].

[29] A. Coogan and S. Profumo arXiv:1705.09664 [astro-ph.HE].

[30] S.-J. Lin, X.-J. Bi, and P.-F. Yin (2018) , arXiv:1801.00997 [astro-ph.HE].

[31] Y.-C. Ding, N. Li, C.-C. Wei, Y.-L. Wu, and Y.-F. Zhou *Journal of Cosmology and Astroparticle Physics* **1906** no. 06, (2019) 004, arXiv:1808.03612 [hep-ph].

[32] L. Randall and W. L. Xu *Journal of High Energy Physics* **2020** no. 5, (May, 2020) . https://doi.org/10.1007%2Fjhep05%282020%29081.

[33] P. von Doetinchem *et al. JCAP* **08** (2020) 035, arXiv:2002.04163 [astro-ph.HE].

[34] M. M. Kachelrieß, S. Ostapchenko, and J. Tjemsland *Journal of Cosmology and Astroparticle Physics* **2020** no. 08, (Aug, 2020) 048–048. https://doi.org/10.1088%2F1475-7516%2F2020%2F08%2F048.

[35] Y.-C. Ding, N. Li, and Y.-F. Zhou *Journal of Cosmology and Astroparticle Physics* **2023** no. 03, (Mar, 2023) 051. https://doi.org/10.1088%2F1475-7516%2F2023%2F03%2F051.

[36] M. Boudaud, Y. Génolini, L. Derome, J. Lavalle, D. Maurin, P. Salati, and P. D. Serpico *Phys. Rev. Res.* **2** no. 2, (2020) 023022, arXiv:1906.07119 [astro-ph.HE].

[37] F. Calore, M. Cirelli, L. DEROME, Y. Genolini, D. Maurin, P. Salati, and P. D. Serpico *SciPost Physics* **12** no. 5, (May, 2022) . https://doi.org/10.21468%2Fscipostphys.12.5.163.

[38] S. Balan, F. Kahlhoefer, M. Korsmeier, S. Manconi, and K. Nippel *Journal of Cosmology and Astroparticle Physics* **2023** no. 8, (Aug., 2023) 052, arXiv:2303.07362 [hep-ph].

[39] A. Shukla, "Light nuclei and antinuclei production in proton-proton interactions," 2023. PhD Thesis, Hawaii U., https://cds.cern.ch/record/2859334, presented 09 May 2023.

[40] H. Fuke *et al. Physical Review Letters* **95** no. 8, (Aug., 2005) 081101, astro-ph/0504361.

[41] K. Abe *et al. Phys. Rev. Lett.* **108** (2012) 131301, arXiv:1201.2967 [astro-ph.CO].

[42] K. Abe *et al. Phys. Rev. Lett.* **108** (2012) 051102, arXiv:1107.6000 [astro-ph.HE].

[43] O. Adriani *et al. Soviet Journal of Experimental and Theoretical Physics Letters* **96** (Jan., 2013) 621–627.

[44] O. Adriani *et al.*, [PAMELA Collab.] *La Rivista del Nuovo Cimento* **40** no. 10, (2017) 473–522, arXiv:1801.10310 [astro-ph.HE].

[45] M. Aguilar *et al. Physical Review Letters* **117** (Aug, 2016) 091103. https://link.aps.org/doi/10.1103/PhysRevLett.117.091103.

[46] K. Sakai *et al. PoS* **ICRC2021** (2021) 123.

[47] K. Sakai *et al. PoS* **ICRC2023** (2023) 134.

[48] A. Berlin, D. Hooper, and S. D. McDermott *Physical Review D* **89** no. 11, (2014) 115022, arXiv:1404.0022 [hep-ph].

[49] A. Boveia *et al.*, "Snowmass 2021 cross frontier report: Dark matter complementarity (extended version)," 2023.

[50] O. Adriani *et al. Nature* **458** (Apr., 2009) 607–609, arXiv:0810.4995.

[51] M. Aguilar *et al. Physical Review Letters* **110** (Apr, 2013) 141102.

[52] L. Accardo *et al. Physical Review Letters* **113** (Sep, 2014) 121101.

[53] R. K. Leane *et al.*, "Snowmass2021 cosmic frontier white paper: Puzzling excesses in dark matter searches and how to resolve them," 2022. https://arxiv.org/abs/2203.06859.

[54] T. Aramaki *et al.*, "Snowmass2021 cosmic frontier: The landscape of cosmic-ray and high-energy photon probes of particle dark matter," 2022. https://arxiv.org/abs/2203.06894.

[55] A. Shukla, A. Datta, P. von Doetinchem, D.-M. Gomez-Coral, and C. Kanitz *Physical Review D* **102** no. 6, (Sep, 2020) . https://doi.org/10.1103%2Fphysrevd.102.063004.

[56] D.-M. Gomez-Coral, A. Menchaca Rocha, V. Grabski, A. Datta, P. von Doetinchem, and A. Shukla *Physical Review D* **98** no. 2, (2018) 023012, arXiv:1806.09303 [astro-ph.HE].

[57] T. Pierog, I. Karpenko, J. M. Katzy, E. Yatsenko, and K. Werner *Phys. Rev.* **C92** no. 3, (2015) 034906, arXiv:1306.0121 [hep-ph].

[58] S. Ostapchenko *Nuclear Physics B Proceedings Supplements* **151** (2006) 147–150, arXiv:astro-ph/0412591 [astro-ph].

[59] T. Sjostrand, S. Mrenna, and P. Z. Skands *Computer Physics Communications* **178** (2008) 852–867, arXiv:0710.3820 [hep-ph].

[60] S. Agostinelli *et al. Nuclear Instruments and Methods in Physics Research A* **506** no. 3, (2003) 250 – 303.

[61] J. Allison *et al. IEEE Transactions on Nuclear Science* **53** (Feb., 2006) 270–278.

[62] A. Galoyan and V. Uzhinsky *Hyperfine Interaction* **215** no. 1-3, (2013) 69–76, arXiv:1208.3614 [nucl-th].

[63] E.-J. Ahn, R. Engel, T. K. Gaisser, P. Lipari, and T. Stanev *Phys.Rev.* **D80** (2009) 094003, arXiv:0906.4113 [hep-ph].

[64] M. Kadastik, M. Raidal, and A. Strumia *Physics Letters B* **683** (2010) 248–254, arXiv:0908.1578 [hep-ph].

[65] V. Abramov, B. Y. Baldin, A. Buzulutskov, V. Y. Glebov, A. Dyshkant, *et al. Soviet Journal of Nuclear Physics* **45** (1987) 845.

[66] R. Scheibl and U. W. Heinz *Physical Review C* **59** (1999) 1585–1602, arXiv:nucl-th/9809092 [nucl-th].

[67] K. Blum, K. C. Y. Ng, R. Sato, and M. Takimoto *Phys. Rev.* **D96** no. 10, (2017) 103021.

[68] M. Kachelrieß, S. Ostapchenko, and J. Tjemsland *European Physical Journal A* **56** no. 1, (2020) 4, arXiv:1905.01192 [hep-ph].

[69] M. Kachelrieß, S. Ostapchenko, and J. Tjemsland *European Physical Journal A* **57** no. 5, (May, 2021) . https://doi.org/10.1140%2Fepja%2Fs10050-021-00469-w.

[70] M. Mahlein, L. Barioglio, F. Bellini, L. Fabbietti, C. Pinto, B. Singh, and S. Tripathy *European Physical Journal C* **83** no. 9, (2023) 804, arXiv:2302.12696 [hep-ex].

[71] F. Bellini and A. P. Kalweit *Physical Review C* **99** no. 5, (2019) 054905, arXiv:1807.05894 [hep-ph].

[72] K. Blum and M. Takimoto *Physical Review C* **99** no. 4, (2019) 044913, arXiv:1901.07088 [nucl-th].

[73] F. Bellini, K. Blum, A. P. Kalweit, and M. Puccio *Physics Review C* **103** (Jan, 2021) 014907. https://link.aps.org/doi/10.1103/PhysRevC.103.014907.

[74] M. A. Lisa, S. Pratt, R. Soltz, and U. Wiedemann *Annual Review of Nuclear and Particle Science* **55** no. 1, (Dec., 2005) 357–402. http://dx.doi.org/10.1146/annurev.nucl.55.090704.151533.

[75] S. Acharya *et al. Physics Letters B* **811** (Dec, 2020) 135849. https://doi.org/10.1016%2Fj.physletb.2020.135849.

[76] D. L. Mihaylov, V. M. Sarti, O. W. Arnold, L. Fabbietti, B. Hohlweger, and A. M. Mathis *European Physical Journal C* **78** no. 5, (May, 2018) . https://doi.org/10.1140%2Fepjc%2Fs10052-018-5859-0.

[77] F. Becattini and U. W. Heinz *Zeitschrift für Physik C Particles and Fields C* **76** (1997) 269–286, arXiv:hep-ph/9702274 [hep-ph]. [Erratum: Z. Phys.C76,578(1997)].

[78] A. Andronic, P. Braun-Munzinger, J. Stachel, and H. Stöcker *Physics Letters B* **697** no. 3, (2011) 203 – 207.

[79] J. Cleymans, S. Kabana, I. Kraus, H. Oeschler, K. Redlich, and N. Sharma *Physical Review C* **84** no. 5, (Nov., 2011) 054916, arXiv:1105.3719 [hep-ph].

[80] Z.-W. Lin, C. M. Ko, B.-A. Li, B. Zhang, and S. Pal *Physical Review C* **72** no. 6, (Dec, 2005) . https://doi.org/10.1103%2Fphysrevc.72.064901.

[81] F.-X. Liu, Z.-L. She, H.-G. Xu, D.-M. Zhou, G. Chen, and B.-H. Sa *Scientific Reports* **12** no. 1, (2022) 1772.

[82] T. Shao, J. Chen, Y.-G. Ma, and Z. Xu *Physical Review C* **105** no. 6, (2022) 065801, arXiv:2205.13626 [hep-ph].

[83] B. Alper, H. Boggild, P. Booth, F. Bulos, L. J. Carroll, G. von Dardel, G. Damgaard, B. Duff, F. Heymann, J. N. Jackson, G. Jarlskog, L. Jonsson, A. Klovning, L. Leistam, E. Lillethun, G. Lynch, G. Manning, M. Prentice, D. Quarrie, and J. M. Weiss *Physics Letters B* **46** (Sept., 1973) 265–268.

[84] W. Gibson, A. Duane, H. Newman, H. Ogren, S. Henning, G. Jarlskog, R. Little, T. Sanford, S. Wu, H. Boggild, B. Duff, K. Guettler, M. Prentice, and S. Sharrock *Lettere al Nuovo Cimento* **21** no. 6, (1978) 189–194.

[85] J. Simon-Gillo *et al.*, [NA44 Collab.] *Nuclear Physics A* **590** (1995) 483C–486C.

[86] T. Armstrong *et al.*, [E864 Collab.] *Physical Review Letters* **85** (2000) 2685–2688.

[87] S. Afanasiev *et al.*, [NA49 Collab.] *Physics Letters B* **486** (2000) 22–28.

[88] T. Anticic *et al.*, [NA49 Collab.] *Physics Review C* **69** (2004) 024902.

[89] S. Adler *et al.*, [PHENIX Collab.] *Physical Review Letters* **94** (2005) 122302.

[90] T. Alexopoulos *et al.*, [Fermilab E735 Collaboration Collab.] *Physics Review D* **62** (Sep, 2000) 072004. https://link.aps.org/doi/10.1103/PhysRevD.62.072004.

[91] A. Aktas *et al.*, [H1 Collab.] *European Physical Journal C* **36** (2004) 413–423.

[92] D. M. Asner *et al. Physical Review D* **75** no. 1, (Jan., 2007) 012009, hep-ex/0612019.

[93] S. Schael *et al. Physics Letters B* **639** no. 3–4, (2006) 192 – 201.

[94] B. I. Abelev *et al.*, [STAR Collab.] *Science* **328** (2010) 58–62.

[95] H. Agakishiev *et al.*, [STAR Collab.] *Nature* **473** (2011) 353.

[96] J. Adam *et al.*, [ALICE Collab.] *Physics Review C* **93** no. 2, (2016) 024917.

[97] J. Adam *et al.*, [ALICE Collab.] *Physics Letters B* **754** (2016) 360–372.

[98] J. Adam *et al.*, [ALICE Collab.] *Nature Physics* **11** no. 10, (2015) 811–814.

[99] S. Acharya *et al.*, [ALICE Collab.] *European Physical Journal* **C77** no. 10, (2017) 658.

[100] S. Acharya *et al.*, [ALICE Collab.] *Physics Letters B* **794** (2019) 50–63.

[101] J. Adam *et al.*, [STAR Collab.] *Nature Physics* **16** no. 4, (2020) 409–412.

[102] J. Adam *et al. Physical Review C* **99** no. 6, (2019) 064905, arXiv:1903.11778 [nucl-ex].

[103] A. Kittiratpattana, M. F. Wondrak, M. Hamzic, M. Bleicher, C. Herold, and A. Limphirat *European Physical Journal A* **56** no. 10, (Oct, 2020) . https://doi.org/10.1140%2Fepja%2Fs10050-020-00269-8.

[104] S. Acharya *et al. European Physical Journal C* **82** no. 4, (Apr, 2022) . https://doi.org/10.1140%2Fepjc%2Fs10052-022-10241-z.

[105] H. Adhikary *et al.*, [NA61/SHINE Collab.], "Report from the NA61/SHINE experiment at the CERN SPS," Tech. Rep. CERN-SPSC-2022-034, SPSC-SR-319, CERN, Geneva, 2022. https://cds.cern.ch/record/2839856.

[106] A. Aduszkiewicz *et al.*, [NA61/SHINE Collab.] *European Physical Journal* **C77** no. 10, (2017) 671, arXiv:1705.02467 [nucl-ex].

[107] A. Aduszkiewicz *et al.*, [NA61/SHINE Collab.] *Eur. Phys. J.* **C77** no. 2, (2017) 59, arXiv:1610.00482 [nucl-ex].

[108] A. Aduszkiewicz *et al.*, [NA61/SHINE Collab.] arXiv:2006.02153 [nucl-ex].

[109] H. Adhikary *et al. European Physical Journal C* **83** no. 10, (Oct., 2023) 919, arXiv:2302.04593 [nucl-ex].

[110] H. Adhikary *et al.*, [NA61/SHINE Collab.] arXiv:2312.13706 [hep-ex].

[111] A. Borucka, [NA61/SHINE Collab.] *Moscow Univ. Phys. Bull.* **77** no. 2, (2022) 178–179.

[112] M. Gazdzicki, [NA61/SHINE Collab.], "Report from the NA61/SHINE experiment at the CERN SPS," tech. rep., CERN, Geneva, 2019. https://cds.cern.ch/record/2692088.

[113] A. Acharya *et al.*, [NA61/SHINE Collab.], "Report from the NA61/SHINE experiment at the CERN SPS," Tech. Rep. CERN-SPSC-2020-023, SPSC-SR-278, CERN, Geneva, 2020. https://cds.cern.ch/record/2739340.